Insights into isotherm making in the sorptive removal of fluoride from drinking water

S. Ayoob, A.K. Gupta *

Environmental Engineering Division, Department of Civil Engineering, Indian Institute of Technology, Kharagpur 721302, India

Abstract

The defluoridation research has thrown up many technologies, with adsorption as a popular alternative, especially among fluoride endemic habitations of the developing world. In the endeavor to develop novel adsorbents for defluoridation, the adsorption potential of hardened alumina cement granules (ALC) were examined through isotherm fitting. Though the adsorbent showed enhanced adsorption capacity at higher fluoride concentration ranges, the errors associated with linearization in isotherm fitting were also found to be increasing. The propagation of these errors was more prominent in Dubinin–Radushkevich and Langmuir models but negligible in Freundlich. The χ^2 analysis, used to correlate the equilibrium experimental data and the isotherm models, also suggested poor correlations at higher fluoride concentration ranges for all the models. The procedure of linear and nonlinear regression through optimization of error functions rendered the 'best-fit' model and optimum model parameters, through sum of normalized error (SNE) values. Though ALC exhibited maximum monolayer adsorption capacity of 34.36 mg g^{-1} in concentration variation studies of fluoride in the range of 2.5–100 mg l^{-1} in synthetic water, it got reduced to 10.215 mg g^{-1} in dose variation studies and further to 0.9358 mg g^{-1} in natural ground water. Though Langmuir appeared as the best-fit model in terms of R^2 in synthetic studies of different fluoride concentrations, the procedure of linear and nonlinear regression demonstrated that Freundlich was the best-fit. The nonlinear χ^2 analysis together with minimum SNE values convincingly demonstrated that the equilibrium studies with dose variations of ALC offers more reliable isotherm parameters than those with high fluoride concentrations. The sorption of fluoride by ALC appeared endothermic with Freundlich adsorption capacity parameter increased from 0.5589 to 0.9939 l g^{-1} in natural water and 3.980–7.5198 l g^{-1} in synthetic water systems for a rise in temperature from 290 to 310 K. The study deviates from conventional methodologies of relying solely on R^2 values in selecting 'best-fit' isotherm model, and basically demonstrates how the optimum model parameters like 'adsorption capacity' evolves through linear and nonlinear regression using error functions.
© 2007 Elsevier B.V. All rights reserved.

1. Introduction

The presence of fluoride in drinking water at low concentrations is considered essential in guarding against dental caries [1]. Accordingly, a permissible guideline range of 0.5–1.0 mg l^{-1} of fluoride has been recommended in drinking water [2]. However, its excess presence in drinking water generates waves of concern as it imparts dental, skeletal and crippling skeletal fluorosis in human [3]. Adsorption is regarded as an important

cost-effective technique most widely used for excess fluoride removal from aqueous solution especially in developing countries where impact of the issue is highly intense and touching. The success of this process mainly hinges on the development and application of economically viable, technically feasible, and socially acceptable adsorbents. The criteria for selection of an adsorbent mainly include its potential (adsorption capacity) for fluoride removal and the cost. In this direction, though a number of adsorbents with very high potential have had been developed (Table 1), paradoxically, only few of them like activated alumina were reported successful at the implementation level [4]. But the most recent revelations on the fluoride adsorption capacity of activated alumina deserve special mention. Though high fluoride removal capacity of alumina (~4–15 mg g^{-1}) is

* Corresponding author. Tel.: +91 3222 283428; fax: +91 3222 282254.
  E-mail addresses: ayoobtkm@yahoo.co.in (S. Ayoob),
akgupta@iitkgp.ac.in (A.K. Gupta).

Table 1
The fluoride adsorption capacities of various adsorbents with corresponding fitting isotherms

S. no.	Name of adsorbent	Dose of adsorbent (g l⁻¹)	Fluoride concentration (mg l⁻¹)	Removal (%), maximum adsorption capacity (mg g⁻¹)	Adsorption isotherm applied	References
1	Activated bauxite	25	25	95%	Freundlich	[30]
2	Activated alumina	25	25	95%	Freundlich	[30]
3	Activated alumina	–	20	84%, 4.0	Langmuir	[31]
4	Lanthanum impregnated silica gel	10.0	10.45	99.97%, 3.80	Langmuir	[32]
5	Alum sludge	8.0	25	100%, 5.394 mg g⁻¹	Langmuir	[33]
6	Aluminum impregnated carbon	–	4.0	1.07 mg g⁻¹	Langmuir	[34]
7	Mixed rare earth oxides	4.0	50.0	12.50 mg g⁻¹	Langmuir	[35]
8	Red mud	2.0	21.28	82%	Langmuir	[36]
9	α-Alumina	–	–	2.73 mg g⁻¹	Langmuir	[37]
10	Activated alumina	4	13.8	96%, 1.45 mg g⁻¹	Langmuir and Freundlich	[38]
11	Aligned carbon nanotubes	–	15	4.5 mg g⁻¹	Freundlich	[39]
12	Lanthanum impregnated cross-linked gelatin	4.0	20.0	21.28 mg g⁻¹	Langmuir	[40]
13	Hydrous ferric oxide	20.0	1000	16.5 mg g⁻¹	Freundlich	[8]
14	Al^{3+} exchanged zeolite	10–80		37.54 mg g⁻¹	Freundlich	[41]
	La^{3+} exchanged zeolite			59.11 mg g⁻¹	Freundlich	
15	Refractory grade bauxite	10.0	4.0	80%	Langmuir	[42]
16	Titanium rich bauxite	1.0	10.0	3.8 mg g⁻¹	Langmuir	[43]
17	Brick powder	10.0	5.0	51–56%	Freundlich	[44]
18	MgAl–CO₃ layered double hydroxides	7.5	5.0–2500	319.8 mg g⁻¹	Langmuir–Freundlich	[9]

reported in literature [5], field experiences demonstrated that it is often around 1 mg g⁻¹ only [6]. This essentially suggests that the assessment of adsorption capacity parameter is crucial for reliable field applications of an adsorbent.

Generally, the adsorption capacity (mg of fluoride adsorbed/g of adsorbent) is assessed on the basis of equilibrium sorption data generated by continuously mixed batch reactor (CMBR) studies, through 'best-fitting' of isotherm models. So, the fitting of experimental data to adsorption isotherm models turns most important, as it dictates the optimum model parameters. The CMBR laboratory studies for equilibrium sorption data can be conducted either by changing the concentrations of adsorbate (fluoride) or the dose of adsorbent. However, most of the reported isotherm studies are on concentration variations in synthetic samples (de-ionized or distilled water laced with fluoride), which lose the 'real-life' flavors and characteristics of natural samples. In general, apart from concentrations of adsorbate, the pH of the medium and the presence of other competing ions drastically alter the adsorption capacity of the adsorbents in aqueous solutions [5]. So, it is rational to suggest that the adsorption capacity reported on synthetic samples cannot be a reliable representation of its actual scavenging potential in field applications as demonstrated in the case of activated alumina.

Of late, the limited success of adsorbents in field applications raises apprehensions over the use of adsorption capacity (generated from equilibrium data) as a measure of their effectiveness in drinking water treatment. Generally, the adsorption capacity of the adsorbent will increase with increasing influent concentrations, till it reaches a maximum. Obviously, the isotherm studies performed for a higher range of fluoride concentrations will show higher capacity than those at moderate or lower ranges. However, this maximum capacity may not describe the media behavior at typical influent fluoride concentrations. It is reported that the concentrations of fluoride in ground waters of the worst affected countries like India are in the range of 0.5–48.0 mg l⁻¹ [7]. Nonetheless, as shown in Table 1, it is not uncommon to encounter isotherm studies performed at fluoride concentrations of 1000 mg l⁻¹ [8] and even upto 2500 mg l⁻¹ [9]. Whereas, in isotherm studies of natural samples, this approach (of concentration variations) becomes inappropriate as concentration of fluoride in ground water remains constant. So, in defluoridation studies dealing with natural ground water, it is only possible to have isotherm studies with dose-variations of adsorbents. This further (in general) suggests the irrelevance of concentration variation studies in sorption process for removing (pollutants like) fluoride from aqueous systems.

Another important aspect is the propagation of errors in the process of isotherm making. It was suggested that the transformations of nonlinear isotherm equations to linear forms for isotherm making, implicitly alter their error structure and may violate the error variance and normality assumptions of standard least squares [10,11]. As a result, many recent studies on adsorption indicate that it is highly inappropriate to use correlation coefficients (R^2) of linear regression in selecting the best-fitting isotherm, rather suggest nonlinear regression to obtain its optimum model parameters [12–14]. So, it is rational to expect that the optimum adsorption capacity parameter generated through

a process of linear and nonlinear regression would be more reliable for field applications. The performance of the adsorbent for field application may also be evaluated in all seasons, as equilibrium data as a function of temperature, may aid in understanding the thermodynamics of sorption process.

This paper basically researches into various aspects of isotherm making in assessing the adsorption capacity of a newly developed adsorbent, alumina cement granules (ALC). The objective is centered on how the adsorption capacity parameter of the isotherm models could be developed through linear and nonlinear regression, by examining the effects from concentration of adsorbate, dose of adsorbent, nature and temperature of the medium.

2. Theory

2.1. Adsorption isotherms

Adsorption isotherms are used for understanding the mechanism and quantifying the distribution of the adsorbate between the liquid phase and solid adsorbent phase at equilibrium during the adsorption process. The Langmuir [15], Freundlich [16] and Dubinin–Radushkevich [17] isotherm models were most commonly used in sorption studies. However, all these isotherms might reasonably be called "empirical" because they are not derived from molecular or thermodynamic principles and are purely descriptive.

2.1.1. Langmuir isotherm (LI)

Though, originally derived for the solid–gas interface, the general kinetic features of the Langmuir model (Eq. (1)) are equally applicable for any interface.

$$q_e = \frac{q_{max} b C_e}{1 + b C_e} \tag{1}$$

where q_e is the amount of adsorbate adsorbed at equilibrium per unit weight of adsorbent (mg g^{-1}), C_e the equilibrium solute concentration (mg l^{-1}), q_{max} and b are Langmuir constants which are related to saturated monolayer adsorption (mg g^{-1}) and binding energy or affinity parameter of the sorption system, respectively. The corresponding linear form of the equation is

$$\frac{1}{q_e} = \frac{1}{b q_{max} C_e} + \frac{1}{q_{max}} \tag{2}$$

This empirical model assumes uniform surface having equivalent adsorption sites with no lateral interactions between the adsorbed species. Thus, LI refers to homogeneous sorption, where each molecule has equal sorption activation energy [12] with no transmigration of the adsorbate in the plane of the surface. Thus, the three essential premises of LI are monolayer coverage, adsorption site equivalence and independence. However, the second and the third assumptions may not hold because solutes will have a tendency to adsorb onto more active sites where pre-adsorbed molecules could be easily displaced. As a result, this type of (heterogeneous) adsorption often leads to an 'island adsorption', which in turn, results unsatisfactory data fitting by the Langmuir isotherm [18].

The Langmuir equation includes two constants each of which has a clear physical meaning: 'b' is the equilibrium constant for the adsorption process expressed in terms of the ratio of the adsorption and desorption rate constants and hence is directly related to the binding energy ($b \propto e^{-\Delta H/RT}$, where ΔH is the net enthalpy change). q_{max} is the adsorption limit obtained at high solute concentrations when $bC_e \gg 1$, and q_e shows a zero order dependence on the solute concentration. For very low values of C_e, the term $b\,C_e \ll 1$, this reduces the hyperbolic equation to a linear equation first order in solute concentration as

$$q_e = kC_e \tag{3}$$

where

$$k = q_{max} b \tag{4}$$

This is analogous to Henry's Law. Graphically, a plateau characterizes the Langmuir isotherm. Therefore, at equilibrium, a saturation point is reached where no further adsorption can occur. The affinity parameter (b) is best estimated from the slope of the adsorption isotherm at very low concentrations. However, this slope gives the product '$q_{max}b$' and not just 'b'. In order to separate these two parameters, it is necessary to know the adsorption maximum 'q_{max}', and this can only be estimated with precision from data at very high concentrations where the slope of the isotherm approaches zero. If data are restricted to an intermediate range of concentration, then they may be fitted very well, but it will be difficult to separate q_{max} and b; the values of which will show a high negative correlation and correspondingly, high standard errors [19].

2.1.2. Freundlich isotherm (FI)

Like the Langmuir model, the Freundlich model (Eq. (5)) also has an empirical origin, but is extremely useful for experimentally determining the adsorption capacity (k_f).

$$q_e = k_f C_e^{1/n} \tag{5}$$

where n is a constant representing adsorption intensity and is always greater than unity.

The corresponding linear form of the equation is

$$\ln q_e = \ln k_f + \frac{1}{n} \ln C_e \tag{6}$$

The Freundlich equation is a special case for heterogeneous surface energies in which the binding energy term b, in the Langmuir equation, varies as a function of the surface coverage q_e, essentially due to variations in heats of adsorption [20]. This model agrees quite well with the Langmuir model at moderate concentrations. However, unlike the Langmuir equation, it does not reduce to a linear adsorption expression at low solute concentrations (Henry's Law) but remains convex to the concentration axis. It also does not agree with the Langmuir equation at very high solute concentrations since n must reach a finite limiting value when the surface is fully covered.

2.1.3. Dubinin–Radushkevich isotherm (DRI)

The D–R isotherm (Eq. (7)) is more general than Langmuir since it does not assume a homogeneous surface or constant sorption potential. The DR isotherm has a Gaussian energy distribution and it does not predict Henry's law at low pressure, but has been used successfully at high solute activities [21]. It often fits data well in the intermediate range of concentrations but in its basic form has unsatisfactory asymptotic properties [19]. Generally, it was applied to distinguish between the physical and chemical adsorption of metal ions:

$$q_e = Q_m \exp(-k_{ad}\varepsilon^2) \tag{7}$$

where k_{ad} is a constant related to adsorption energy, Q_m the theoretical saturation capacity (mg g^{-1}), and ε is the Polanyi potential and is given by

$$\varepsilon = RT \ln\left(1 + \frac{1}{C_e}\right) \tag{8}$$

where R is the universal gas constant (8.314×10^{-3} kJ/(mol K)) and T is the absolute temperature (K). The corresponding linear form of Eq. (7) is

$$\ln q_e = \ln Q_m - k_{ad}\varepsilon^2 \tag{9}$$

The Langmuir and Freundlich isotherms models are said to suffer from two major drawbacks [22]. Firstly, the model parameters obtained are usually appropriate for a particular set of conditions and that cannot be used as a prediction model for another. Secondly, these models are unable to provide a fundamental understanding of ion adsorption. However, even though many other isotherm models have been developed, both LI and FI still remain as the two most commonly used equilibrium adsorption equations (Table 1). The continued application of these models undoubtedly reflects their ability to fit a wide variety of adsorption data quite well, but it may also partly reflect the appealing simplicity of the isotherm equations and the ease with which their adjustable parameters can be estimated.

2.2. Linear and nonlinear regression minimizing error functions

Generally, the assumption inherent in the development of the isotherm models limits their applications under different (diverse) conditions. Thus, in the absence of a generally applicable single model, a comparison of different models, and selection of a 'best-fitting' model (to the respective data set), becomes inevitable. Of late, the coefficient of regression (R^2) values had have been the only criterion for selecting this best fit. Naturally, the isotherm giving an R^2 value closest to unity is deemed to provide the best fit [23]. Since making of the isotherm involves formulation of linear transforms (LTFM) of the basic model equations, the inherent bias resulting from this process, prompted researchers for nonlinear regression. So, attempts have been made in selecting best-fit isotherm and its optimum parameters using both linear and nonlinear regressions of transformed isotherms by minimizing a series of error functions [13,23–28], though for fluoride sorption, the first time.

To examine the effect of different error criteria in fitting the respective data set to the isotherm equations and to enhance the optimization process, five different error functions were selected. This include the sum of squares of errors (SSE), the sum of absolute errors (SAE), the average relative error (ARE), the hybrid fractional error function (HYBRID), and the Marquardt's percent standard deviation (MPSD) as described elsewhere [12,14,27]. These error functions were evaluated and minimized in each case across the respective data set using the *solver* add-in with Microsoft's spreadsheet, Excel 2003 (Microsoft Corporation). Since the minimization of each of the error functions renders corresponding set of isotherm parameters, for selecting the optimum isotherm parameters among them, 'sum of the normalized errors' (SNE) were used [23]. This normalization procedure allows direct combination of these scaled errors and identifies the optimum parameter set by its minimum SNE values. Further, since the different error functions selected are presumed to cover a reasonably wide selection, it is plausible that the distribution of the experimental data does not give excessive weight either to high or low concentration ranges.

2.3. χ^2 analysis of nonlinear regression

The difference in the axial settings of linear equations (of individual isotherm models) will alter the result of a linear regression process, thereby influencing the determination of the model parameters. Whereas, in the nonlinear χ^2-analysis suggested by Ho [13], all isotherms are being compared on the same abscissa and ordinate, thus avoiding such errors of linearization. The equivalent mathematical statement was

$$\chi^2 = \sum \frac{(q_{exp} - q_{cal})^2}{q_{cal}} \tag{10}$$

So, if data from model were similar to the experimental data, χ^2 would be a small number and vice versa.

3. Experimental

3.1. Adsorbent

The adsorbent (ALC), selected for the present research, was prepared from a commercially available high alumina cement. The rich presence of alumina and calcium, whose (established) potential for fluoride scavenging was instrumental in selection of this adsorbent. Initially, slurry was prepared by adding distilled water to 1 kg of high alumina cement at a water–cement ratio of ~0.3. The slurry was kept at ambient temperature for 2 days for setting, drying and hardening. This hardened paste was cured in water for 5 days. After curing, it was broken, granulated, sieved to geometric mean size of ~0.212 mm, and kept in airtight containers for use.

3.2. Adsorbates, reagents and stock solutions

All chemicals and reagents used in this study were of analytical grade. NaF (Merck) was used for preparation of the standard

Table 2
Characteristics of natural ground water (collected from Baliasingh Patna, Kurda district, Orissa, India)

Characteristic parameter	Quantitative value (mg l^{-1})
Fluoride	8.65
pH	6.9 ± 0.4
Acidity	0.0
Alkalinity	260
Chloride	165
Total hardness	145
Total organic carbon	59.08
Total phosphorous	0.032
Silicate as SiO$_2$	39.22
Boron	0.33
Sodium	14.00
Potassium	2.00
Ammonia nitrogen	0.328
Salinity	0.30*

* Salinity is expressed in PSS (practical salinity scale).

fluoride (adsorbate) stock solution in double distilled water. All synthetic fluoride solutions for adsorption and analysis were prepared by appropriate dilution of the stock solution in de-ionized (DI) water. Only plastic wares were used for handling fluoride solution and is not prepared in or added to glass containers. All plastic ware were washed in dilute HNO$_3$ acid bath and rinsed thoroughly with DI water prior to use. The natural fluoride rich drinking water was collected from Baliasingh Patna, a fluoride endemic village (Kurda district, Orissa state) in India. The characteristics of ground water are illustrated in Table 2.

3.3. Analysis/instrumentation

Expandable ionAnalyzer EA 940 with Orion ionplus (96-09) fluoride electrode (Thermo Electron Corporation, USA), using TISAB III buffer was used for fluoride measurement. The pH measurement was done by a Cyber Scan 510 pH meter (Oakton Instruments, USA). A temperature controlled orbital shaker (Remi Instruments Ltd., Mumbai, India) was used for agitation of the samples in CMBR studies. A high precision electrical balance (Mettler Toledo, Model AG135) was used for weight measurement. Nephelo turbidity meter (Systronics, Model 131) was used for turbidity measurement. The elemental composition of ALC combined with oxygen was determined by Energy Dispersive X-ray (EDX) analysis (Oxford ISIS-300 model) by quantitative method in two iterations using ZAF correction, at a system resolution of 65 eV, and results were normalized stoichiometrically. The surface area of the adsorbent was determined by the BET method at liquid nitrogen temperature using FlowSorb II 2300 (Micrometrics Instruments corporation, USA).

3.4. Characterization of adsorbent

The elemental composition of ALC (combined with oxygen) obtained from EDX showed presence of Al$_2$O$_3$ (78.49%), CaO (15.82%), SiO$_2$ (5.39%), and Fe$_2$O$_3$ (0.30%). The bulk density, pH of zero point charge (pHzpc), and BET surface area were 2.33 g cm^{-3}, 11.32 and 4.385 m^2 g^{-1}, respectively. The pH at

zero point charge of ALC was determined as per the method suggested by Noh and Schwarz [29]. Different quantities of ALC were placed in 10 ml solutions of 0.1 M NaCl (prepared in pre-boiled water) in various bottles and kept in the thermostat shaker for overnight continuous agitation. The equilibrium pH values of these mixtures were measured and limiting value is reported as pHzpc.

3.5. Isotherm studies

The equilibrium adsorption tests of fluoride on ALC were carried out in continuously mixed batch reactors. Polyethylene bottles (Tarson Co. Ltd., India) of 150 ml capacity with 50 ml of fluoride solutions of desired concentration and pH were used. ALC was added as per dose requirements and bottles were shaken in the orbital shaking incubator at 230 ± 10 rpm. Synthetic samples of the same concentration (8.65 mg l^{-1}) and pH (6.5–7) as that of natural water were prepared in DI water. In concentration variation studies of synthetic samples, a fixed ALC dose (2 g l^{-1}) was maintained in all fluoride concentrations. In dose variation studies, the ranges selected was 3–13 g l^{-1} in natural, and 1–3 g l^{-1} in synthetic waters, respectively. The effect of temperature on fluoride adsorption was studied at 290, 300 and 310 K. All other experiments were carried out at room temperature (∼300 K). The bottles were taken out from the shaker after 3 h and the content was filtered using Whatman No-42 filter paper to separate the sorbent and filtrate. From the filtered sample of each batch reactor, 10 ml was taken for analysis and determination of residual fluoride.

3.5.1. Adsorption capacity of adsorbent
The adsorption capacity (experimental) of ALC, i.e. the amount of fluoride adsorbed per unit mass of the adsorbent at any time t (q_t, mg g^{-1}), can be calculated as

$$q_t = \frac{C_0 - C_t}{m} V \tag{11}$$

where C_0 and C_t are the fluoride concentrations in solution (mg l^{-1}) initially and at any time (t), respectively, m the mass of ALC (g) and V is the volume (l) of the solution. In Eq. (11), when $C_t = C_e$ (fluoride concentrations remaining in the solution at equilibrium in mg l^{-1}), $q_t = q_e$ (equilibrium adsorption capacity in mg g^{-1}).

4. Results and discussion

4.1. Effects of adsorbate concentration

The visual inspection of the experimental equilibrium data and the isotherm models (Fig. 1(a)–(d)) indicates comparable uptake of fluoride by ALC. An enhanced uptake of fluoride by ALC at higher concentration is visible for LI and DRI models (with a tendency to tail off at very high concentrations), whereas FI provides identical uptake pattern. The shape of the fluoride isotherm data suggests that both FI and LI models would provide a reasonable fit to the experimental data at all con-
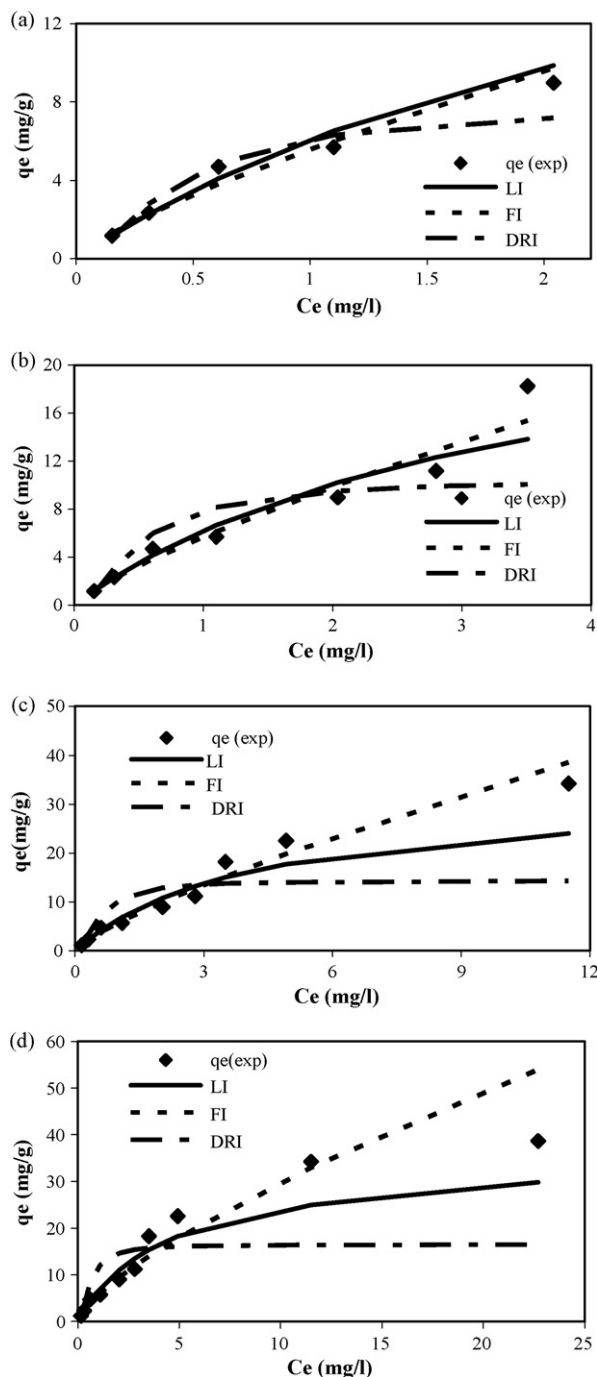
Fig. 1. (a) A comparison of the experimental data and various isotherm models in the concentration range of 2.5–20 mg l^{-1} of fluoride in synthetic samples. (b) A comparison of the experimental data and various isotherm models in the concentration range of 2.5–40 mg l^{-1} of fluoride in synthetic samples. (c) A comparison of the experimental data and various isotherm models in the concentration range of 2.5–80 mg l^{-1} of fluoride in synthetic samples. (d) A comparison of the experimental data and various isotherm models in the concentration range of 2.5–100 mg l^{-1} of fluoride in synthetic samples.

centration ranges compared to DRI. It can be observed that (Table 3) LI fit the data better at all ranges of concentration with very high consistent values of R^2 (>0.995). The FI also makes identical fitting, though with slightly lower R^2 values. However, the FI fitting becomes better towards higher concen-

tration ranges with a steady increase in R^2 from 0.9738 to 0.9955. Thus, adsorption of fluoride by ALC derives significant in the concentration ranges studied, as it deviates from the notion that FI normally fits better at low concentrations and LI at higher concentrations.

As cited above, this traditional approach of determining the isotherm parameters by linear regression of LI and FI models appears to give very good fits to the experimental data as their respective R^2 values are very high (Table 3). Thus, purely from the comparison of R^2 values, the linearized Langmuir isotherm would be expected to provide a 'better fit' for the experimental data than the linearized Freundlich, at all concentration ranges. But, as pointed out earlier, due to the inherent bias resulting from linearization, alternative single-component parameter sets were determined by nonlinear regression. The isotherm parameters of the individual models were selected based on the minimum SNE values (in bold Table 4) obtained by minimizing the respective error function across the desired concentration. It can be seen that SNE values obtained by linear regression are maximum for LI model at all concentration ranges indicating the significance of nonlinear regression in evaluating the model parameters. Whereas, the SNE values of FI model are minimum at all concentration ranges in linear regression indicating the reliability of the respective model and its parameters. So, it is too obvious that regardless of the error function chosen and the range of concentrations selected, the Freundlich isotherms renders in lower absolute error values through SNE, and will be the 'best-fit' as against the corresponding Langmuir isotherms, suggested by linear regression. Further, the relatively higher values of χ^2 (Table 3), together with its sharp increase towards the higher fluoride concentration ranges (irrespective of the isotherm models), indicating that the quality of correlation falls off rapidly, supports the significance of nonlinear regression in this concentration variation study. This increase is more prominent in DRI and LI, which indicates the growing discrepancy between model predictions and the experimental data, and clearly suggests the inability of these models in predicting the fluoride sorption by ALC. The minimum values of χ^2 in FI compared to LI and DRI models, indicates more similarity between model predictions and the experimental data by FI, further supports its choice as the 'best-fit'. But still, the magnitude of its χ^2 values, clearly pointing to the prominence of discrepancy between the model and experimental data at higher fluoride ranges. This may reduce confidence in model predictions, and leave enough concern on the precision of the isotherm parameters suggested by even the 'best-fit' model.

As expected, the results of this study suggest that the adsorption capacity of ALC increases with increase in the range of adsorbate (fluoride) concentrations selected. The effect of concentration of fluoride in the magnitude of adsorption capacity parameters was maximum in DR isotherm, very high in Langmuir, but negligible in Freundlich (Table 3). Since most of the reported isotherm studies follows Langmuir model (Table 1), it indicates that those adsorbents developed using equilibrium data generated at higher fluoride concentration ranges, need not be representing its actual fluoride adsorption capacity. Further, it indicates that the comparison of adsorption potentials obtained

Table 3
Isotherm model parameters, R^2, and χ^2 values in natural and synthetic systems at different temperatures

Isotherm model	Model parameters and R^2	Range of fluoride concentrations (mg l^{-1}) synthetic samples at 300 K				Temperature of observations and nature of samples					
		2.5–20	2.5–40	2.5–80	2.5–100	290 K		300 K		310 K	
						Natural	Synthetic	Natural	Synthetic	Natural	Synthetic
LI	R^2	0.9952	0.9955	0.9954	0.9955	0.8768	0.9877	0.9215	0.9599	0.9672	0.9918
	b	0.329	0.2958	0.244	0.230	1.0336	0.8245	15.22	1.0471	10.696	1.3036
	q_{maxm} (mg g^{-1})	24.57	27.17	32.57	34.36	1.0779	9.09	0.9358	10.215	1.164	12.658
	χ^2	0.2732	1.8874	7.2521	9.4317	0.0513	0.4834	0.0156	0.1356	0.0211	0.0656
FI	R^2	0.9738	0.9776	0.9843	0.9955	0.9275	0.9937	0.9364	0.9734	0.9391	0.9878
	$1/n$	0.7755	0.7939	0.7839	0.7248	0.3342	0.5569	0.1022	0.5959	0.1553	0.6287
	K_f (l g^{-1})	5.593	5.676	5.682	5.610	0.5589	3.980	0.825	5.1924	0.9939	7.5198
	χ^2	0.2987	1.1159	1.9953	7.2599	0.0224	0.0181	0.0080	0.0802	0.0239	0.0493
DRI	R^2	0.9588	0.8729	0.7821	0.7536	0.7440	0.9048	0.8826	0.9278	0.9463	0.4651
	Kad	0.0791	0.0955	0.1135	0.1215	0.2046	0.0864	0.0136	0.1291	0.0171	0.0572
	Q_m (mg g^{-1})	7.776	10.46	14.39	16.510	0.9157	6.9302	0.9157	6.1978	1.140	8.2137
	χ^2	0.6049	8.0358	39.696	60.836	0.0811	1.809	0.0191	2.9909	0.0258	0.1538

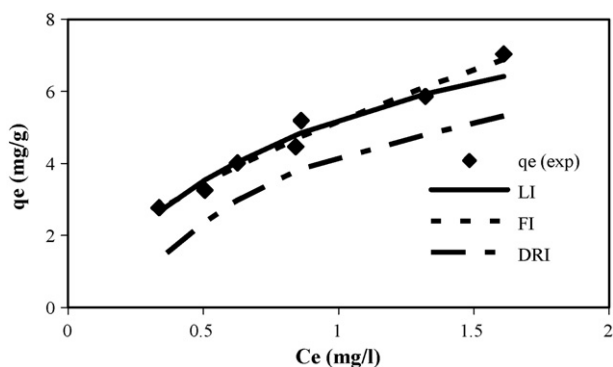
Fig. 2. A comparison of the experimental data and various isotherm models in synthetic samples under dose variation study.

Fig. 4. The Freundlich isotherm model fitting at different temperatures in both natural and synthetic systems.

under different fluoride concentration ranges, to highlight the effectiveness of adsorbents, turns inappropriate and meaningless.

4.2. Effects of adsorbent dose

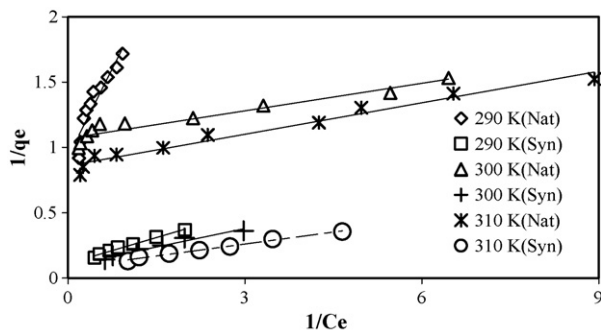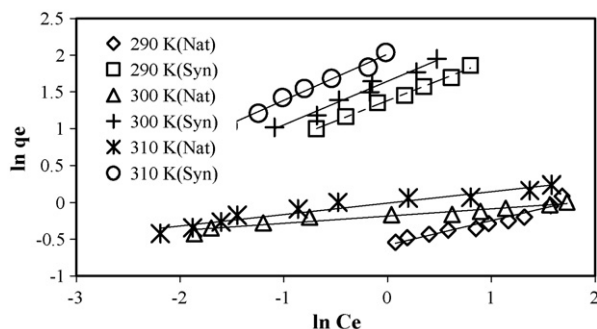The fitting of isotherm in equilibrium sorption with variation of dose of adsorbent in synthetic sample, clearly contradicts those from concentration studies. The visual inspection of the experimental equilibrium data and the isotherm models (Fig. 2) indicates that both FI ($R^2 = 0.9734$) and LI ($R^2 = 0.9599$) have reasonably good fittings compared to DRI ($R^2 = 0.9278$). Interestingly, all models renders minimum SNE values (Table 4) in linear regression itself (as shown in LTFM column), rendering nonlinear regression insignificant. The very low values of χ^2 (even much less than R^2 in most of the cases) by all isotherm models assure better similarity between model predictions and

Fig. 3. The Langmuir isotherm model fitting at different temperatures in both natural and synthetic systems.
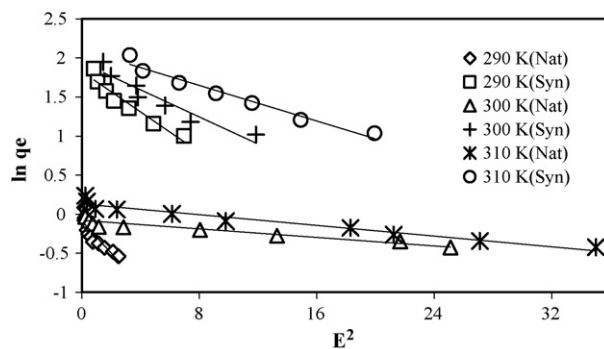

Fig. 5. The D–R isotherm model fitting at different temperatures in both natural and synthetic systems.

Table 4
Tabulation of SNE for isotherm models under different conditions

		LTFM	SSE	SAE	ARE	HYBRID	MPSD
Concentration variation at 300 K							
2.5–20 mg l^{-1}							
SNE	LI	5.000000	4.881777	4.828101	**4.801442**	4.858913	4.818153
	FI	**3.892879**	4.579827	4.743883	4.72238	4.617327	4.788327
	DRI	4.665825	4.888386	4.848317	4.83365	**3.797203**	4.794401
2.5–40 mg l^{-1}							
SNE	LI	4.990531	4.958213	4.974163	4.969901	**4.929129**	4.974992
	FI	**4.74102**	4.998911	4.899273	4.794679	4.818068	4.805519
	DRI	**4.704581**	4.975318	4.942874	4.862059	4.898972	4.866262
2.5–80 mg l^{-1}							
SNE	LI	4.98807	**4.985897**	4.991444	4.992488	4.990477	4.996799
	FI	**3.251215**	4.336985	4.763083	4.800794	4.446493	4.753355
	DRI	**4.705425**	4.981847	4.962313	4.878513	4.909239	4.872515
2.5–100 mg l^{-1}							
SNE	LI	4.995108	**4.994805**	4.996475	4.997450	4.996274	4.99758
	FI	**2.164891**	4.184681	4.508621	4.588042	4.208625	4.509643
	DRI	**4.696117**	4.981335	4.966513	4.880494	4.907350	4.873041
Dose variation in natural water at different temperature							
290 K							
SNE	LI	**1.26788**	4.056719	4.206621	4.165162	4.053183	4.178546
	FI	**1.757752**	3.542966	3.806261	4.348999	3.407867	3.761199
	DRI	**0.804589**	2.680232	4.152842	4.155304	2.678065	2.515826
300 K							
SNE	LI	**1.566206**	4.113045	4.278642	4.267445	4.107082	4.318938
	FI	**3.876257**	4.285933	4.28610	4.802833	4.322426	4.425841
	DRI	**0.58419**	4.021955	4.128816	4.114338	4.01818	4.122546
310 K							
SNE	LI	**1.380078**	4.061019	4.228611	4.227598	4.059646	4.242658
	FI	4.998725	4.976329	4.966906	**4.962299**	4.969168	4.962582
	DRI	**0.355822**	4.007497	4.085689	4.074319	4.005928	4.068946
Dose variation in synthetic water at different temperature							
290 K							
SNE	LI	**0.867907**	3.941634	3.950767	4.050117	3.972073	4.139715
	FI	**3.412766**	4.316424	4.515929	4.502217	4.326029	4.575303
	DRI	5.00000	4.547643	**4.472457**	4.480388	4.560272	4.485741
300 K							
SNE	LI	**1.558044**	4.083988	4.249731	4.250253	4.097009	4.302899
	FI	**4.658318**	4.850895	4.886562	4.873058	4.858223	4.923917
	DRI	**1.624642**	4.136625	4.359413	4.330702	4.120180	4.331568
310 K							
SNE	LI	**1.268763**	4.014825	4.150645	4.155518	4.023045	4.20884
	FI	**2.630046**	4.359419	4.52906	4.462222	4.318238	4.507527
	DRI	**0.424939**	4.007198	4.084937	4.077947	4.00627	4.074567

experimental data. Obviously, Freundlich model (in terms of R^2, χ^2 and SNE values) is the 'best-fit' among the three. Thus, in contrast to the concentration variation results, it clearly establishes the significance and necessity of dose variation studies in determining the 'best-fit' for obtaining optimum isotherm parameters.

4.3. Effects of temperature

The effects of temperature on the entire isotherm models in both natural and synthetic systems (with dose variations) are shown in Figs. 3–5 with respective parameter values in Table 3. As can be seen, both LI and FI have shows reasonable fitting at all temperature ranges in both systems than DRI, though values of R^2 suggests Freundlich fits better. The SNE values (Table 4) for all models at all temperature ranges (except one case in DRI) renders minimum values by linear regression indicating the insignificance of nonlinear regression in isotherm making in (all these) dose variation studies. The minimum values of χ^2 by all isotherms at all temperatures also suggest a better correlation between experimental and model data. In addition to more favorable R^2 and minimum SNE values by linear regression, all error

Table 5
The best-fit isotherm models and optimum isotherm parameters evolved after linear and nonlinear regression minimizing the error functions

Type/nature of adsorption process	Best-fit model selected in terms of R^2	Correlation between experimental and model data in terms of χ^2	Significance of nonlinear regression in terms of SNE	Best-model evolved after linear and nonlinear regression
Concentration variation at 300 K				
2.5–20 mg l^{-1}	LI (q_{max} = 24.57 mg g^{-1}; b = 0.329)	Good	Significant	FI (k_f = 5.593 mg g^{-1}; 1/n = 0.7755)
2.5–40 mg l^{-1}	LI (q_{max} = 27.17 mg g^{-1}; b = 0.2958)	Poor	Significant	FI (k_f = 5.676 mg g^{-1}; 1/n = 0.7939)
2.5–80 mg l^{-1}	LI (q_{max} = 32.57 mg g^{-1}; b = 0.244)	Very poor	Significant	FI (k_f = 5.682 mg g^{-1}; 1/n = 0.7839)
2.5–100 mg l^{-1}	LI (q_{max} = 34.36 mg g^{-1}; b = 0.230)	Very poor	Significant	FI (k_f = 5.610 mg g^{-1}; 1/n = 0.7248)
Dose variation in natural water at different temperature				
290 K	FI (k_f = 0.5589 l g^{-1}; 1/n = 0.3342)	Very good	Insignificant	FI (k_f = 0.5589 l g^{-1}; 1/n = 0.3342)
300 K	FI (k_f = 0.8251 l g^{-1}; 1/n = 0.1022)	Very good	Insignificant	FI (k_f = 0.8251 l g^{-1}; 1/n = 0.1022)
310 K	LI (q_{max} = 1.164 mg g^{-1}; b = 10.696)	Very good	Significant	FI (k_f = 0.9932 l g^{-1}; 1/n = 0.154)
Dose variation in synthetic water at different temperature				
290 K	FI (k_f = 3.981 l g^{-1}; 1/n = 0.5569)	Good	Insignificant	FI (k_f = 3.981 l g^{-1}; 1/n = 0.5569)
300 K	FI (k_f = 5.192 l g^{-1}; 1/n = 0.5959)	Good	Insignificant	FI (k_f = 5.192 l g^{-1}; 1/n = 0.5959)
310 K	LI (q_{max} = 12.658 mg g^{-1}; b = 1.3036)	Good	Insignificant	FI (k_f = 7.5198 l g^{-1}; 1/n = 0.6287)

functions renders minimum error values for Freundlich, imparting more consistency and reliability to its parameters, making it the obvious choice for the 'best-fit' model at all temperature ranges considered. The minimum values of χ^2 in FI compared to other two models, also suggests best correlation between the model and experimental data. It is clear that all isotherm models suggest an enhanced uptake of fluoride by ALC at higher temperatures. The adsorption capacity parameters of all these models (Table 3) records an increase at high temperatures indicating that the process of removal of fluoride is endothermic characterized by a chemisorption mechanism. Also, the reduction in adsorption potential of ALC in the removal of fluoride in natural system (in comparison to synthetic) is evident. As illustrated in Table 3, the reduction is maximized in LI followed by DRI with minimum in FI. It clearly indicates that the adsorption potential rendered by synthetic water studies need not be a reliable measure of the scavenging potential of the adsorbent for field applications. The results of the linear and nonlinear regression process leading to the evolution of best-fit isotherm are summarized in Table 5. It clearly renders the optimum isotherm model parameters which can be used for process design and derivation of sorption breakthrough profiles.

5. Summary

(1) The selection of 'best-fit' isotherm on the basis of mere R^2 values is observed inappropriate in the sorption of fluoride by ALC. An understanding and evaluation of the errors associated in the making of isotherm model is demonstrated essential in selecting the 'best-fit'.
(2) The evaluation of adsorption capacity (through isotherm fitting) using data on synthetic studies based on variations in concentration of fluoride, may render unreliable values, especially when LI is the 'best-fit'.
(3) The procedure of linear and nonlinear regression by minimizing error functions by introducing SNE values is found significant in the analysis of equilibrium adsorption of fluoride by ALC. The SNE values together with χ^2 non-

linear analysis could collectively evaluate the quality of experimental data and render the most optimum isotherm parameters.
(4) The adsorption potential of ALC recorded a reduction in treating natural water in comparison to synthetic water. This turns out to be a fertile area of future research.

6. Conclusion

This study suggests a rethinking on the conventional procedure of isotherm making and selection of 'best-fit' merely by higher coefficient of correlation in linear regression. The nonlinear regression by minimizing error functions deserves merit for selecting the 'best-fit' isotherm model in rendering optimum model parameters. Through χ^2 and minimum SNE values, this study establishes the increasing error variance associated with equilibrium data generated through higher concentrations of adsorbate. Confirming the apprehensions over traditional practice of obtaining adsorption capacity through concentration variations studies, it is suggested that dose variation studies provides more reliable data and are most appropriate. The adsorption capacity of ALC undergoes considerable reduction in treating natural water, compared to synthetic and is influenced by temperature. As described and demonstrated, this sorption studies of fluoride on ALC, suggests a re-orientation in the methodology of assessing the adsorption capacity of adsorbents for 'real-life' applications.

References

[1] WHO, World Health Organization, Geneva, Fluorides, Environmental Health Criteria (2002) 227.
[2] WHO, Guidelines for Drinking-Water Quality: Incorporating First Addendum. vol. 1 Recommendations, 3rd ed., World Health Organization, 20 Avenue Appia, 1211 Geneva 27, Switzerland, 2006, pp. 375–376.
[3] S. Ayoob, A.K. Gupta, Fluoride in drinking water: a review on the status and stress effects, Crit. Rev. Environ. Sci. Technol. 36 (2006) 433–487.
[4] R.K. Daw, Experiences with domestic defluoridation in India, Proceedings of the 30th WEDC International Conference on People-Centred

Approaches to Water and Environmental Sanitation, Vientiane, Lao PDR (2004) 467–473.

[5] J.O. Hao, C.P. Huang, Adsorption characteristics of fluoride onto hydrous alumina, J. Environ. Eng. (ASCE) 112 (1986) 1054–1067.

[6] WHO (World Health Organization), in: J. Fawell, K. Bailey, J. Chilton, E. Dahi, L. Fewtrell, Y. Magara (Eds.), Fluoride in Drinking water, IWA Publishing, Alliance House, 12 Caxton Street, London SW1H 0QS, UK (2006) 41–75.

[7] A.K. Susheela, A Treatise on Fluorosis, Revised 2nd ed., Fluorosis Research and Rural Development Foundation, New Delhi, India, 2003.

[8] S. Dey, S. Goswami, C.U. Ghosh, Hydrous ferric oxide (HFO)—a scavenger for fluoride from contaminated water, Water Air Soil Pollut. 158 (2004) 311–323.

[9] L. Lv, J. He, M. Wei, D.G. Evans, Z. Zhou, Treatment of high fluoride concentration water by MgAl-CO_3 layered double hydroxides: kinetic and equilibrium studies, Water Res. 41 (2007) 1534–1542.

[10] D.A. Ratkowsky, Handbook of Nonlinear Regression Models, Marcel Dekker Inc., New York, 1990.

[11] R.H. Myers, Classical and Modern Regression with Applications, PWS-KENT, 1990, 297–298, 444–445.

[12] S.J. Allen, G. Mckay, J.F. Porter, Adsorption isotherm models for basic dye adsorption by peat in single and binary component systems, J. Colloid Interf. Sci. 280 (2004) 322–333.

[13] Y.S. Ho, Selection of optimum sorption isotherm, Carbon 42 (2004) 2115–2116.

[14] S. Kundu, A.K. Gupta, Arsenic adsorption onto iron oxide-coated cement (IOCC): regression analysis of equilibrium data with several isotherm models and their optimization, Chem. Eng. J. 122 (2006) 93–106.

[15] I. Langmuir, The constitution and fundamental properties of solids and liquids, J. Am. Chem. Soc. 38 (1916) 2221–2295.

[16] H.M.F. Freundlich, Über die adsorption in lösungen, Z. Phys. Chem. 57 (1906) 385–470.

[17] M.M. Dubinin, The potential theory of adsorption of gases and vapors for adsorbents with energetically non-uniform surface, Chem. Rev. 60 (1960) 235–266.

[18] S. Sohn, D. Kim, Modification of Langmuir isotherm in solution systems, definition and utilization of concentration dependent factor, Chemosphere 58 (2005) 115–123.

[19] G.D. Kinnilburgh, General purpose adsorption isotherms, Environ. Sci. Technol. 20 (1986) 895–904.

[20] A.W. Adamson, A.P. Gast, Physical Chemistry of Surfaces, 6th ed., Wiley-Interscience, New York, 1997.

[21] O. Altın, H.O. Ozbelge, T. Dogu, Use of general purpose adsorption isotherms for heavy metal–clay mineral interactions, J. Colloid Interf. Sci. 198 (1998) 130–140.

[22] B. Kasprzyk-Hordern, Chemistry of alumina, reactions in aqueous solutions and its application in water treatment, Adv. Colloid Interf. Sci. 110 (2004) 19–48.

[23] J.F. Porter, G. McKay, K.H. Choy, The prediction of sorption from a binary mixture of acidic dyes using single- and mixed-isotherm variants of the ideal adsorbed solute theory, Chem. Eng. Sci. 54 (1999) 5863–5885.

[24] A. Seidel-Morgenstern, G. Guiochon, Modelling of the competitive isotherms and the chromatographic separation of two enantiomers, Chem. Eng. Sci. 48 (1993) 2787–2797.

[25] A. Malek, S. Farooq, Comparison of isotherm models for hydrocarbon adsorption on activated carbon, Am. Inst. Chem. Eng. J. 42 (1996) 3191–3201.

[26] Y.S. Ho, J.F. Porter, G. McKay, Equilibrium isotherm studies for the sorption of divalent metal ions onto peat: copper, nickel and lead single component systems, Water Air Soil Pollut. 141 (2002) 1–33.

[27] S.J. Allen, Q. Gan, R. Matthews, P.A. Johnson, Comparison of optimised isotherm models for basic dye adsorption by kudzu, Bioresour. Technol. 88 (2003) 143–152.

[28] J.C.Y. Ng, W.H. Cheung, G. McKay, Equilibrium studies for the sorption of lead from effluents using chitosan, Chemosphere 52 (2003) 1021–1030.

[29] J.S. Noh, J.A. Schwarz, Estimation of the point of zero charge of simple oxides by mass titration, J. Colloid Interf. Sci. 130 (1989) 157–164.

[30] W.W. Choi, K.Y. Chen, The removal of fluoride from waters by adsorption, J. AWWA 71 (1979) 562–570.

[31] Y.C. Wu, A. Nitya, Water defluoridation with activated alumina, J. Environ. Eng. Div., ASCE 105 (1979) 357–367.

[32] S.A. Wasay, J.M. Haron, S. Tokunaga, Adsorption of fluoride, phosphate, and arsenate ions on lanthanum-impregnated silica gel, Water Environ. Res. 68 (1996) 295–300.

[33] M.G. Sujana, R.S. Thakur, S.B. Rao, Removal of fluoride from aqueous solutions by using alum sludge, J. Colloid Interf. Sci. 206 (1998) 94–101.

[34] R.L. Ramos, J.O. Turrubiartes, M. Sanchez-Castillo, Adsorption of fluoride from aqueous solution on aluminum impregnated carbon, Carbon 37 (1999) 609–617.

[35] A.M. Raichur, J.M. Basu, Adsorption of fluoride onto mixed rare earth oxides, Sep. Purif. Technol. 24 (2001) 121–127.

[36] C. Yunus, K. Esengul, E. Mustafa, Removal of fluoride from aqueous solution by using red mud, Sep. Purif. Technol. 28 (2002) 81–86.

[37] R.J.L. Bahena, A.R. Cabrera, A.L. Valdivieso, R.H. Urbina, Fluoride adsorption onto α-Al_2O_3 and its effect on the zeta potential at the alumina-aqueous electrolyte interface, Sep. Purif. Technol. 37 (2002) 1973–1987.

[38] S. Ghorai, K.K. Pant, Investigations on the column performance o f fluoride adsorption by activated alumina in a fixed bed, Chem. Eng. J. 98 (2004) 165–173.

[39] H.Y. Li, S. Wang, A. Cao, D. Zhao, X. Zhang, C. Xu, Z. Luan, D. Ruan, J. Liang, D. Wu, W. Wei, Adsorption of fluoride from water by amorphous alumina supported on carbon nanotubes, Chem. Phys. Lett. 350 (2003) 412–416.

[40] Y. Zhou, C. Yu, Y. Shan, Adsorption of fluoride from aqueous solution on La^{3+} impregnated cross-linked gelatin, Sep. Purif. Technol. 36 (2004) 89–94.

[41] S.M. Onyango, Y. Kojima, O. Aoyi, C.E. Bernardo, H. Matsuda, Adsorption equilibrium modeling and solution chemistry dependence of fluoride removal from water by trivalent-cation-exchanged zeolite F-9, J. Colloid Interf. Sci. 279 (2004) 341–350.

[42] D. Mohapatra, D. Mishra, S.P. Mishra, R.G. Chaudhury, R.P. Das, Use of oxide minerals to abate fluoride from water, J. Colloid Interf. Sci. 275 (2004) 355–359.

[43] N. Das, P. Pattanaik, R. Das, Defluoridation of drinking water using activated titanium rich bauxite, J. Colloid Interf. Sci. 292 (2005) 1–10.

[44] A.K. Yadav, C.P. Kaushik, A.K. Haritash, A. Kansal, N. Rani, Defluoridation of groundwater using brick powder as an adsorbent, J. Hazard. Mater. 128 (2006) 289–293.